three freeze-pump-thaw cycles. Irradiation at 77 K with the Xe arc lamp and Corning O-52 cutoff filter ($\lambda > 340$ nm) for 10 h, followed by thawing of the glass, converted the diazirine completely into products. The product mixture was subjected to preparative VPC: 4 ft × $^1/_4$ in., 10% Ov-101 on Chrom P 60/80, RT = 3.5 and 12 min, respectively, for 1,2-dichloro-1,2-dimethoxyethane (**8**) and 1,4-dichloro-1,4-dimethoxy-2,3-diazabuta-1,3-diene (**9**) at 85 °C; ^{1}H NMR spectra identical with those reported in ref 14; IR **8** (NaCl, neat) 3015, 2975, 2945, 2890, 2835, 1655, 1450, 1222, 1193, 1157, 1108, 995, 932, 842, and 796 cm^{-1}; IR **9** (CS_2) 3010, 2990, 2960, 2940, 2820, 1625, 1440, 1255, 1212, 1168, 1090, 1010, and 799 cm^{-1}.

Methoxychlorocarbene (3): IR (N_2 matrix, after photolysis of **4** for 33 h with $\lambda = 370$ nm) 2975 w, 1475 m, 1465 m, 1445 m, 1439 m, 1309 vs, 1299 m, 1140 s, 947 s, 840 m, 810 w, 773 vs, 690 m, 451 m, 400 m, and 394 m cm^{-1}.

Methoxychlorocarbene-d_3 (10): IR (N_2 matrix, after photolysis of **5** for 2 h with $\lambda = 370$ nm) 2180 w, 1362 m, 1329 vs, 1305 vw, 1071 m, 1050 m, 950 s, 925 w, 805 m, 794 vw, 777 w, 769 w, 749 s, 669 m, 434 m, 383 m, and 377 w cm^{-1}.

[^{18}O]Methoxychlorocarbene (11): IR (N_2 matrix, after photolysis of **6** for 6 h with $\lambda = 370$ nm) 2975 w, 1462 m, 1446 m, 1435 w, 1277 s, 1267 m, 1135 m, 920 m, 820 m, 803 m, 793 w, 770 s, 683 m, 441 m, 394 m, and 389 w cm^{-1}.

Acknowledgment. We are grateful to the Donors of the Petroleum Research Fund, administered by the American Chemical Society, for partial support of this work and the Camille and Henry Dreyfus Foundation for generous support of this work. The low-temperature apparatus and IR spectrometer were partially funded by NSF (CHE 8117318). We also thank Dr. T. Clark, Universität Erlangen-Nurnberg, for communication of unpublished calculations and Prof. J. Liebman, University of Maryland, for very helpful discussions and preprints.

Structure and Exchange Behavior of Cryptand 111 and Its Inside Protonated Products

H.-J. Brügge,[†] D. Carboo,[†] K. von Deuten,[†] A. Knöchel,*[†] J. Kopf,[†] and W. Dreissig[‡]

Contribution from the Institut für Anorganische und Angewandte Chemie, Universität Hamburg, D-2000 Hamburg 13, and the Institut für Kristallographie, Freie Universität Berlin, D-1000 Berlin 33, West Germany. *Received April 1, 1985*

Abstract: The structure of the cryptand 111 (**1**) and its inside protonated species [111-H]$^+$ **2** and [H-111-H]$^{2+}$ **3** have been studied by infrared spectroscopy. X-ray crystal structures of all three compounds are also presented and discussed in correlation with the IR data. The structure of **1** is complicated by the existence of disorder not encountered in **2** and **3**. The encapsulated protons in **2** and **3** are covalently bonded to the nitrogens, whereby the NH in **2** is weaker than in **3**, as evidenced by their distances (91.6 and 84.4 pm in **2** and **3**, respectively). The exchange behavior of **2** and **3** has been investigated with the help of exchange reactions of the tritiated analogues [111-T]$^+$ and [T-111-T]$^{2+}$. The results are discussed with respect to the IR data and the crystal structures. It is concluded that **3** is much more stable than **2**. **3** resists in different aqueous solutions an exchange of the encapsulated protons and therefore is suitable for the fixation of tritium.

1. Introduction

Macrocyclic diamines including cryptands are known to yield, on treatment with acid, inside as well as outside protonation products. This property can be attributed to the inherent ability of the ligands to exist in any one of the three possible exo-endo conformations first discussed by Simons and Park.[1]

In the large flexible compounds, e.g., cryptand 222, the rate of interconversion of the conformers into one another is quite fast, and the endo-endo (in,in) configuration is assumed to be predominant[2] although other conformations may also occur depending on the substitution in the bridge, as evidenced by the pyridine-substituted cryptand 222 with flattened nitrogens.[3] The mechanism of protonation in the flexible ligands is of the direct proton-transfer type and may involve diffusion of the attacking proton into the molecular cavity and/or conformational change from "in" to "out" followed by protonation.[2]

Small- and medium-ring bicyclic diamines on the other hand may be geometrically strained and less flexible. This imposes restrictions on the interconversion either completely or partially. The first case leads to a situation in which the nitrogens are exo-exo, e.g., in 1,4-diazabicyclo[2.2.2]octane (DABCO).[4] The second case provides a mixture of exo-exo, exo-endo, and endo-endo. The protonation reactions are therefore complicated, and in some cases, they do not follow the classical mechanism. A comprehensive evaluation of experimental data in this respect warrants knowledge of the structures of these ligands, and this is scarce.

Alder and Session, having synthesized a large number of medium-ring bicyclic amines, could obtain the crystal structures of only the 1,6-diazabicyclo[4.4.4]tetradecane and its monoprotonated ion.[5-7] Lehn and Dye prepared the cryptand 111 and studied its structure as well as the kinetics and thermodynamics of protonation by means of high-resolution NMR.[8-10]

Figure 1 shows the structural formula of the cryptand 111 and its inside protonation forms. The ligand exists predominantly in the in-in conformation with an interconversion energy of 40.96 kJ/mol. Protonation is slow and yields outside as well as inside protonated ions. Especially the inside protonation species **2** and **3** resist neutralization under severe conditions.

[†] Institut für Anorganische und Angewandte Chemie.
[‡] Institute für Kristallographie.

(1) Simmons, H. E.; Park, C. H. *J. Am. Chem. Soc.* **1968**, *90* 2428.
(2) Pizer, R. *J. Am. Chem. Soc.* **1978**, *100* 4239. Cox, B. G.; Knop, D.; Schneider, H. *J. Am. Chem. Soc.* **1978**, *100* 6002.
(3) Newcome, G. R.; Majestic, V.; Fronczeck, F.; Atwood, J. L. *J. Am. Chem. Soc.* **1979**, *101* 1047.
(4) Basolo, F. *Coord. Chem. Rev.* **1968**, *3* 213.
(5) Alder, R. W.; Sessions, R. B. *J. Am. Chem. Soc.* **1979**, *101* 3651.
(6) Alder, R. W.; Moss, R. E.; Sessions, R. B. *J. Chem. Soc., Chem. Commun.* **1983**, 997.
(7) Alder, R. W.; Orpen, A. G.; Sessions, R. B. *J. Chem. Soc., Chem. Commun.* **1983**, 999.
(8) Cheney, J.; Lehn, J.-M. *J. Chem. Soc., Chem. Commun.* **1972**, 487.
(9) Cheney, J.; Kintzinger, J. K.; Lehn, J.-M. *Nouv. J. Chim.* **1978**, *2* 411.
(10) Smith, P. B.; Dye, J. L.; Cheney, J.; Lehn, J.-M. *J. Am. Chem. Soc.* **1981**, *103* 6044.

0002-7863/86/1508-0107$01.50/0

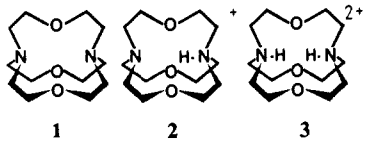

1 2 3

Figure 1. Cryptand 111 and its inside protonation forms.

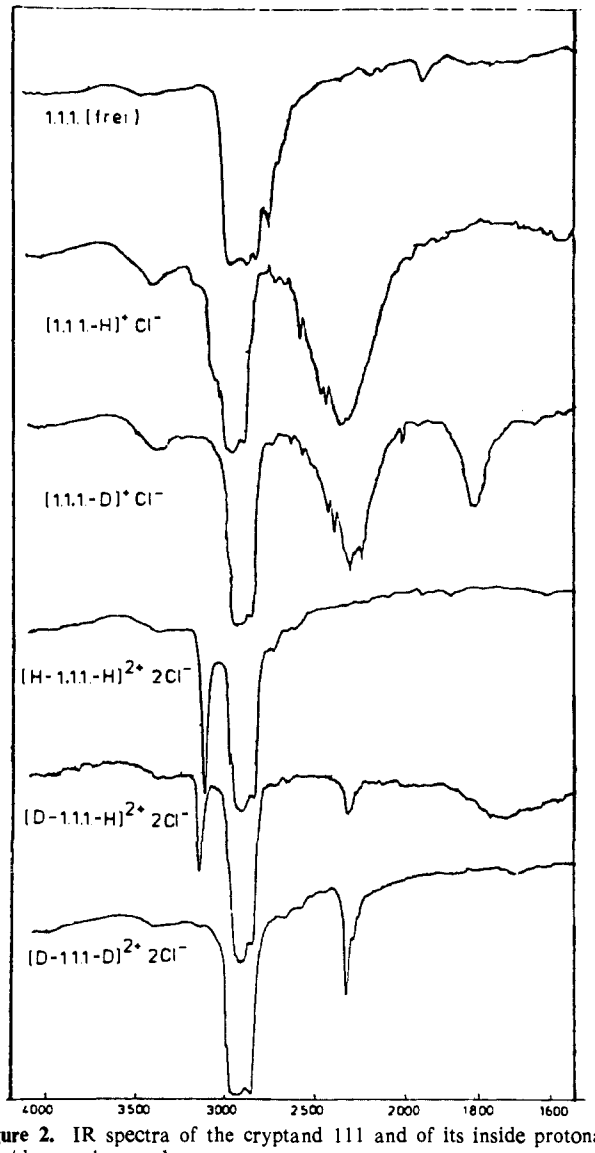

Figure 2. IR spectra of the cryptand 111 and of its inside protonation/deuteration products.

We now report the IR spectra and X-ray crystal structures of **1**, **2**, and **3** as well as the exchange behavior of **2** and **3**.

2. Results and Discussions

2.1. Structure of Cryptand 111. The IR spectra of **1**, **2**, and **3** together with the spectra of the deuterated complexes are shown in Figure 2. The accompanying anion in **2** and **3** is Cl^-.

The IR spectrum of **1** shows in the 2700–2800-cm^{-1} region the Bohlmann bands.[11] These bands, also present in the spectra of the larger cryptands, arise as a result of an α-CH_2 hydrogen being antiperiplanar to at least a lone pair of the nitrogen.

Spectra of **1**, run in $CDCl_3$ according to the method of Lord and Siamwiza,[12] display a relatively strong satellite at 2236 cm^{-1} in addition to the ν_{C-D} at 2254 cm^{-1} for $CDCl_3$.

The shift of 17 cm^{-1} to lower frequencies is small compared to that of, for example, cryptand 222 (64 cm^{-1}), where a larger proportion of the nitrogen lone pairs have exo conformation and

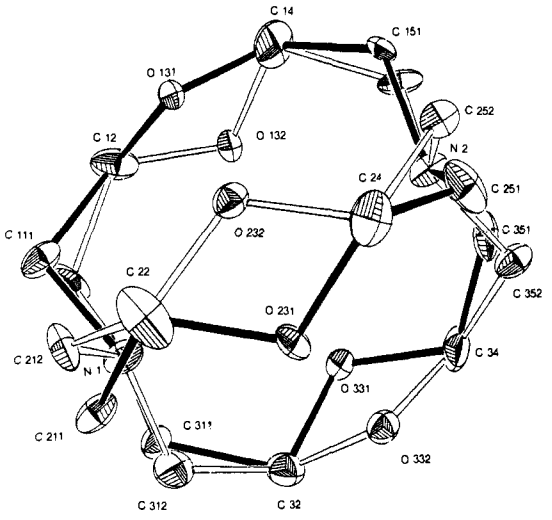

Figure 3. ORTEP plot of **1**.

Table I. Selected Bond Angles, Distances, and Torsion Angles of **1** (Estimated Standard Deviations Are in Parentheses)

bond angles, deg		bond distances, pm	
N1–C111–C12	118.7 (1.5)	N1–C111	145.5 (2)
C12–O131–C14	110.1 (1)	C111–C12	133.2 (2)
C111–C12–O131	117.9 (7)	C111–H111	107.8 (9)
O131–C14–C151	98.9 (0.8)	C111–C112	78 (2)
C14–C151–N2	114.1 (4)	O131–C12	142.4 (1.4)
		O131–O132	148.3 (1)
H111–C111–N1	110.3 (5)	C211–C22	136.2 (4)
H121–C12–O131	110.3 (5)	C311–C31	141.1 (0.1)
torsion angles, deg		**torsion angles, deg**	
N1–C111–C12–O131	58.7 (2)	C22–O231–C24–C251	152.7 (1)
C111–C12–O131–C14	138.8 (1)	O231–C24–C251–N2	−71.1 (1)
C12–O131–C14–C151	150.6 (1)	N1–C311–C32–O331	55.5 (2)
O131–C14–C151–N2	−74.1 (1)	C311–C32–O331–O34	133.9 (1)
N1–C211–C22–O231	55.8 (1)	C32–O331–O34–O351	153.3 (1)
C211–C22–O231–O24	133.9 (1)	O331–C34–C351–N2	−76.5 (1)
LSQ distances, pm		**LSQ distances, pm**	
N1 from C111–C211–C311	22.9	N2 from C151–C251–C351	30.9
N1 from C112–C121–C312	31.3	N2 from C152–C252–C352	23.5

therefore are accessible to hydrogen bonding. The proportion of endo, inaccessible nitrogens in **1** must be large. Furthermore, the ν_{COC} of **1** is split into two bands at 1100 and 1140 cm^{-1}, indicating differently oriented ether functions.

The low temperature crystal structure of **1** is shown in Figure 3. The structure displays statistical disorder in the positions of the carbon atoms directly bonded to the nitrogens as well as in the positions of the oxygens. For each of these atoms, double maxima are found in the electron density difference synthesis. Similar disorder problems are encountered in the structure determination of cyclododecane,[13] the experimental data of which satisfied two molecular models. The distance between the two maxima for each carbon atom is ~75 pm and for the oxygens the two maxima are further apart by ~150 pm, leading to a system of two intertwined molecules. This is expressed in the ORTEP plot (Figure 3) by the opened and closed lines. Each molecule in the system is convertible into the other by a C2 rotation.

As a result of the disorder, there are around each nitrogen six carbon sites (three pairs) through which two mean planes can be drawn. From Table I, it can be seen that N2 is 309 pm and 23.5 pm away from the C151–C251–C351 and C152–C252–C352

(11) Bohlmann, F. *Chem. Ber.* **1958**, *91* 2157.
(12) Lord, R. C.; Siamwiza, N. M. *Spectrochim. Acta* **1975**, *3117* 1381.
(13) Dunitz, J. D.; Sheare, H. M. M. *Helv. Chim. Acta* **1960**, *43* 18.

planes, respectively. This confirms the inward pyramidization at the nitrogen. The C–N–C angles are between 115° and 120° and indicate a certain flattening at the nitrogens. Perhaps the actual structure is an endo–exo type with the molecules arranged in pairs of mirror images, i.e., exo–endo/endo–exo. This may also explain the disorder observed and the interconvertibility. Another way of rationalizing the observed disorder may be to assume a rapid conformational change, which in the solid state is not likely.

Considering one molecule, the conformations of the three bridges as deduced from the torsion angle are identical. Six of the 12 torsion angles are about 60° (synclinal) and the rest about 160° (antiperiplanar). The high percentage of the energetically unfavorable skew partial conformation may contribute to the rigidity of **1**.

All the ether oxygens lie outside the C–C–O–C–C plane and subtend an angle of 50–70°. The resulting O–O′ and N–O contact distances are 379 (1) and 279 (1) pm, respectively. Contrary to an estimation of Lehn,[8] the N–N′ distance is 388 (2) pm, indicating the absence of an eventual N–N′ interaction as postulated for medium-sized bicyclic diamines.[14]

In general bond distances are within theoretical range, with only C111–C12, C112–C12, and C311–C32 ranging between 133 and 144 pm, and as such the bond distances are very short. Also, the minimum contact distances between hydrogens on adjacent C atoms as computed with the *calculated* hydrogen positions are above 206 pm.

On the whole, **1** is highly symmetrical but strained. As a medium-sized bicyclic diamine, the introduction of heteroatoms should not cause large changes in the conformation.[13]

The increase of the electron density in the molecular cavity (resulting from oxygen and nitrogen lone pairs) has given cause to repulsive effects. **1** therefore assumes such conformation that would limit the repulsive forces in the cavity and relax the molecule. The elongation in the N–N′ axis coupled with the oxygens being directed away from the cavity only serve the purpose of relaxing the molecule. It may, however, cause large rotational movements in the skeleton, leading to disorder. This assertion is supported by the detailed studies of Lehn and co-workers of the solution structure of **1** by NMR techniques.[9] They showed that contrary to ^{13}C spectra, ^{1}H spectra depict a temperature-dependent conversion from the *AA′–XX′* system (292 K) to the *AB–XY* system (165 K). This was thought rather to be due to freezing out torsional motions around the single bonds in the bridges as against movements due to in–out isomerism.

2.2. Structure of Monoprotonated 111. Contrary to **1**, the Bohlmann bands are absent in the IR spectrum of **2**·Cl^-. Since **2** is monoprotonated, the complete disappearance of these bands may be due to hydrogen bonding to the second nitrogen, a situation which is incompatible with the long N–N′ distance of 388 pm found in **1**. The NH stretching frequency appears in the 2500–2200-cm^{-1} region. Upon deuteration of **1** with 99.99% DCl, this band is shifted to 1800 cm^{-1} with an isotopic factor of 1.3. The broadness and position, compared to that of normal ν_{N-H}, can be rationalized with the additional hydrogen bonding not only to the second nitrogen but also to the oxygens. Similar bonds, found in the spectra of nonplanar bicyclic amines, e.g., spateine perchlorate,[15] were interpreted to arise from intermolecular hydrogen bonding in which H is symmetrically located between the nitrogen atoms. A prerequisite is, however, a N–N′ distance not exceeding 280 pm as found in crystal structures[7,16] as well as neutron diffraction studies[17] of N^+–H···N systems. The N–H stretching vibrations of such systems are broad, intensive, and in all cases below 1000 cm^{-1}. Hence, the encapsulated proton in **2** is probably asymmetrically located. However additional interactions to the oxygens may assist in hydrogen transfer between the nitrogens. This also explains the shift (20 cm^{-1}) of the ν_{C-O} to lower wavenumbers.

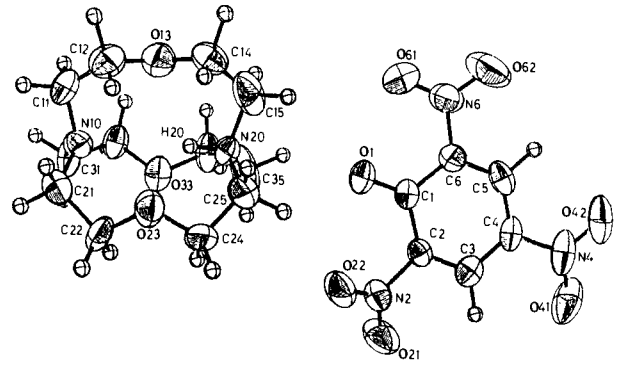

Figure 4. Crystal structure of **2** picrate.

Table II. Selected Angles and Distances of **2** (Estimated Standard Deviations Are Given in Parentheses)

angles, deg		distances, pm	
C31–N10–C11	114.8 (0.3)	N10–H20	274.9 (0.6)
C31–N10–C21	115.0 (0.3)	O13–H20	231.5 (0.6)
C21–N10–C11	113.9 (0.3)	O23–H20	220.9 (0.6)
C35–N20–C25	109.6 (0.3)	O33–H20	235.9 (0.6)
C25–N20–C15	111.7 (0.3)	N20–O1	334.8 (0.6)
C35–N20–C15	112.3 (0.3)	N20–N10	360.4 (0.6)
H20–N20–C15	108.8 (0.3)	N20–H20	91.4 (0.6)
		N20–O13	275.5 (0.6)
		N20–O23	274.2 (0.6)
		N20–O33	276.2 (0.6)

The crystal structure of **2** picrate is shown in Figure 4. Selected angles and distances are given in Table II. The molecule depicts the endo–endo conformation as demanded by the spectroscopic data. H20 is in the molecular cavity and bonded covalently to N20, making the vicinities of both nitrogens unequal. Whereas C–N20–C is about 110° and ideally tetrahedral, C–N10–C is about 115° and approaches the planar configuration. Conclusively, it can be said that the protonation has accentuated the inward pyramidization of N20, leaving N10 largely unaffected and causing the N–N′ distance to contract by 28 pm from 388 to 360.4 pm. It is interesting to note further that the same amount of decrement was registered for the inside monoprotonated 1,6-diazabicyclo[4.4.4]tetradecane.[7] The N–N′ distance in **2** is, however, large compared to the 253 pm of this compound and lends further support to the acclaimed asymmetrical localization of the proton in **2**.

The slight decrease of the NO contact distances from 285 pm in **1** to 275 pm in **2** means that in spite of the relatively long N–N′, the most meaningful interaction to H20 must come from N10 and not from the oxygens. This is in keeping with the arguments advanced by Lehn et al.[9] regarding the localization of the encapsulated proton. Their ^{1}H NMR studies in solution revealed a proton which is exchanging fast between the nitrogen sites, the exchange being too fast on the NMR time scale. Since the crystal structure favors a definitely covalent NH bond and the N–N′ is relatively long, one would have to evoke the intermediation of the oxygens to explain these observations. It must be emphasized, however, that the relationships in solution are not necessarily identical with those prevailing in the solid state.

The presence of a positive charge in the cavity reduces the high density (from the heteroatoms). On going from **1** to **2**, the 12 ring (containing O33 and O23) becomes more chairlike and the bond angles relax toward normal values, so that large torsional motions are minimized and the disorder disappears. **2** is, however, not completely strainless as can be deduced from some bond angles especially around N10 (see Table II). Apparently, the single positive charge is not sufficient to totally neutralize the high

(14) Alder, R. W.; Arrowsmith, R. J.; Casson, A.; Sessions, R. B.; Heilbronner, E.; Kovac, B.; Huber, H.; Taagepera, W. *J. Am. Chem. Soc.* **1981**, *103* 6137.

(15) Skolic, J.; Wiewierowski, M.; Kruger, P. J. *J. Mol. Struct.* **1974**, *5* 461.

(16) Quick, A.; Williams, D. J.; Borak, B.; Wood, J. L. *J. Chem. Soc., Chem. Commun.* **1974**, 891.

(17) Roziere, I.; Belin, C.; Lehmann, M. S. *J. Chem. Soc., Chem. Commun.* **1982**, 388.

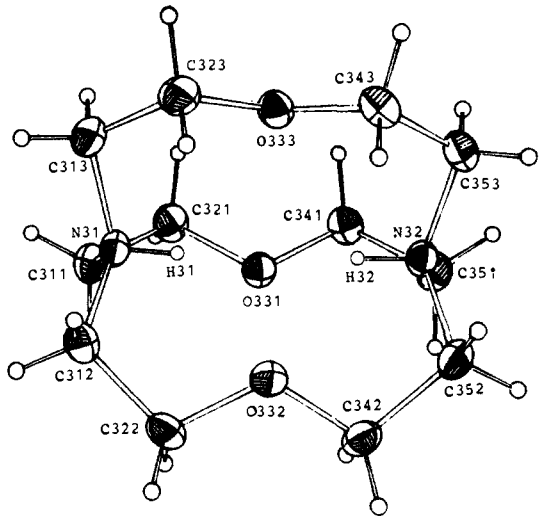

Figure 5. Structure of **3**.

electron density in the molecular cavity. The three oxygens are still directed 20–35° away from the cavity.

2.3. Structure of Diprotonated 111. The ν_{NH} of **3**·2Cl⁻ is intensive and appears at 3140 cm^{-1} (Figure 2). This assignement is based on comparison with the spectrum of the deuterated analogue, which depicts an ν_{N-D} at 2350 cm^{-1}. For an NH$^+$ capable of undergoing hydrogen bonding with the ether oxygens, the sharpness is not easily understood, except that the said interactions are in reality very weak. Quagliano et al.[18] found analogous results, when they inserted a transition-metal cation into the intramolecular NH$^+$···N system of protonated 1,4-diazabicyclo[2.2.2]tetraoctane (DABCO). The second protonation in **3** must have destroyed the intramolecular NH$^+$···N interaction, thus augmenting the electronic pull at the nitrogens. The NH bond becomes stronger with higher vibrational frequency.

Compared to **2**, one would expect the oxygens to increase their interaction with the encapsulated protons, simply because of the increased charge. An inspection of the ν_{C-O-C} reveals a shift of 30 cm^{-1} to smaller wavenumbers. This is relatively small and testifies to the weak nature of the NH···O interaction, which on the other hand confirms the general notion that nonlinear hydrogen bonds are weak.

Figure 5 shows the crystal structure of **3**; selected angles and torsion angles are listed in Table III. The macrocation **3** depicts an endo–endo conformation in which the two nitrogens are equivalent.

The inward pyramidization as a result of the encapsulation of two protons is higher than in **2**. To accommodate the two protons in the cavity, however, the N–N′ distance has increased to 390 pm compared to 360.4 pm in **2** and 388 pm in **1**. There is a marked constriction of the molecule along the C2 plane, causing the oxygens to draw nearer. The O–O′ and the N–O contact distances decrease steadily on going from **1** to **2** to **3**:

	1	2	3
N–O, pm	292	275	272
O–O′, pm	379	368	324

The repulsion of the ether oxygens from the molecular cavity encountered in **1** and to a lesser extent in **2** appears completely absent, and all the ether oxygens are pointing into the molecular cavity. Both N–H distances in **3** (84.6 pm) are relatively short and equal and correlate well with the IR data in respect to the absorption frequency. Interactions to the ether oxygens cause less weakening of the bonds as compared to the N–H in **2** (NH = 91.4 pm).

On the whole, **3** has gained in stability as a result of the diprotonation. The torsion angles have not changed; there is a balance of synclinal (60°) and antiperiplanar (160°) configurations, but the bond angles and distances have all normalized to stabilize **3**.

Table III. Selected Distances, Angles, and Torsion Angles of **3** (Picrate)$_2$ (Estimated Standard Deviations Are Given in Parentheses)

angles, deg		distances, pm	
C331–N31–C313	111.5 (1)	N31–N32	391 (0.4)
C311–N31–C312	113.7 (1)	N31–O331	271.3 (0.4)
C312–N31–C313	116.5 (1)	N32–O331	271.9 (0.4)
C351–N32–C353	112.4 (1)	N32–O333	272.3 (0.4)
C351–N32–C353	113.2 (1)	O331–O332	322.2 (0.7)
C352–N32–C353	118.1 (1)	O331–O333	327 (0.3)
		O332–O333	322.7 (0.5)
C1–C2–O3	123.5 (0.8)	N11–O11	385 (0.7)
O3–C2–H21	118.6 (5)	N32–O21	383 (0.6)
C1–C2–H21	117.6 (5)		
C2–C1–H111	124.5 (4)	O3–C2	134.6 (0.9)
H111–C1–H112	78.4 (6)	C2–C1	136.4 (1.1)
H112–C1–C2	123.7 (4)	C2–H21	89.6 (7.6)
		C1–H111	120.2 (8)
		C1–H112	102.2 (8)

torsion angles, deg			
N31–C311–C321–O331	54.17 (0.5)	C321–O331–C341–C351	165.6 (0.3)
C311–C321–O331–C341	−162.0 (0.3)	O331–C341–C351–N32	55.3 (0.4)
N31–C312–C322–O332	54.3 (0.4)	C322–O332–C342–C352	166.8 (0.4)
C312–C322–O332–C342	−165.4 (0.4)	O332–C342–C352–N32	53.2 (0.4)
N31–C313–C323–O333	54.0 (0.5)	C323–O333–C343–C353	167.1 (0.4)
C313–C323–O333–C343	−163.7 (0.4)	O333–C343–C353–N32	−56.1 (0.5)

2.4. Exchange Behavior of 2 and 3. From the thermodynamic point of view, one would expect **2** to be more stable than **3** since the positive charge of H20 in **2** can be more widely distributed. Neutralization experiments conducted by Lehn et al. support this: **2** cannot be deprotonated unless the cryptand is destroyed. On the other hand, one of the protons in **3** can be removed by a base only under extremely rigorous conditions.[7-9] These results, however, do not provide any informations on the exchange behavior of the protonated species. Especially the complexation of macrocyclic polyether with alkali ions is known to yield kinetically unstable products. The encapsulated cations are exchanging continuously. The thermodynamic data only describe the equilibrium state and do not cover the exchange reaction. The exchange behavior is of fundamental importance in the application of the macrocyclic polyether in the field of isotope enrichment by chemical exchange processes.[19,20] Similar behavior is found in the protonation product of the larger cryptands, and this is exploited in the enrichment of deuterium or tritium.[21]

We have therefore investigated the exchange behavior of **2** and **3** by radiochemical techniques using tritiated products.

In conducting these reactions, **2** and **3** were allowed to exchange at 298 and 337 K for 24 h according to the following equations:

$$[111\text{-T}]^+ + H_2O \rightleftharpoons [111\text{-H}]^+ + HTO$$

$$[T\text{-}111\text{-T}]^{2+} + H_2O \rightleftharpoons [T\text{-}111\text{-H}]^{2+} + HTO$$

$$[T\text{-}111\text{-H}]^{2+} + H_2O \rightleftharpoons [H\text{-}111\text{-H}]^{2+} + HTO$$

Apart from H_2O, different acid and base concentrations were employed. The filtrate was separated by freeze-drying, and the tritium activities of both filtrate and residue were measured by liquid scintillation counting. The results of the experiment at 298

(18) Quagliano, J. V.; Banerjee, A. K.; Goedken, V. L.; Vallareno, L. M. *J. Am. Chem. Soc.* **1970**, *92* 482.
(19) Knöchel, A.; Wilken, R.-D. *J. Am. Chem. Soc.* **1981**, *103* 5707.
(20) Cahen, J. M.; Dye, J. L.; Popov, A. I. *J. Chem. Phys.* **1975**, *79* 1289.
(21) German Patent P3202776 DE-OS (1983).

Table IV. Exchange Behavior of $[111\text{-}T]^+$ and $[T\text{-}111\text{-}T]^{2+}$

tritiated species	solvent	filtrate(%)	residue(%)
$[111\text{-}T]^+Cl^-$	H_2O	35 ± 2	65 ± 3
	1 N HCl	9.95 ± 2	93.6 ± 4
	0.1 N HCl	9.51 ± 3	88.7 ± 5.6
	0.01 N HCl	9.04 ± 2	90.83 ± 4.3
	1 N KOH	19.9 ± 2.5	75.6 ± 5.0
	0.1 N KOH	15.2 ± 2.0	83.79 ± 2.4
	0.01 N KOH	9.08 ± 3.6	90.93 ± 4.8
$[T\text{-}111\text{-}T]^{2+}2Cl^-$	H_2O	0.19 ± 0.11	97.84 ± 4
	1 N HCl	2.1 ± 1.0	99.48 ± 4.4
	0.1 N HCl	0.24 ± 0.1	98.7 ± 5.0
	0.01 N HCl	0.31 ± 0.1	101.03 ± 5.1
	1 N KOH	2.1 ± 1.33	97.85 ± 5.0
	0.1 N KOH	3.65 ± 3.0	93.5 ± 5.5
	0.01 N KOH	4.6 ± 1.5	98.3 ± 7.0

K are summarized in Table IV.

The extent of exchange in **2** at 298 and 373 K is in all solvents and especially in H_2O very high and contradicts, at a first glance, the results of neutralization experiments. **3** depicts very low exchange as expected. Even at elevated temperatures, the exchange rate is very low.

A plausible explanation to the apparent discrepancy in the case of **2** can be found by considering the structural advantages and disadvantages of **2** and **3**. As already described above, all ether oxygens in **3** are directed into the molecular cavity and interact optimally with the encapsulated protons. This is illustrated by the IR spectra as well as by the short NH distance of 84.6 pm. Exchange reactions require either a conformational change, which exposes the encapsulated protons,[22] or an entry of the incoming proton into the cavity. The former involves a high activation energy of 105 ± 8 kJ/mol as shown by Lehn.[9] A neutralization by this route is therefore very slow. The latter is enhanced by hydrogen bond formation to the oxygens. In **3**, these are directed into the cavity and not accessible to attack by protons from outside. In **2**, however, the oxygens are directed 20–35° away from the cavity, and in addition, the unprotonated, nearly sp^2-hybridized N10 can be attacked by electrophiles, e.g., protons, as illustrated by Figure 6. Such an attack at an oxygen site or N10 could initiate, by way of a push–pull mechanism, an in–out conformational change under formation of O–H or out N–H bond. The intermediate protonation compensates for the required activation energy. Finally, T^+ is eliminated and **2** is formed after a second change of the conformations to endo–endo. Lehn has shown that such intermediate out-protonated species do have very short half-lives and readily convert into the more stable in-protonated species. The conversion is, however, strongly dependent on the acidity of the medium.[10]

Comparison of the amounts of exchange in the various aqueous solutions reveals further that in general, the exchange is higher for all the base concentrations. Therefore, in addition to the exchange, there is a neutralization which is probably the dominating process, but in all cases, **3** is more stable than **2**.

In concluding, we note that both **2** and **3** are quaternary ammonium salts, having their protons nicely concealed in the cavity, whereby the degree of shielding is higher for the protons in **3** than for that in **2**. In spite of the existing possibility in **2** for the asymmetrically located proton to undergo weak hydrogen bonding, it must be emphasized that **2** has more vulnerable sites, rendering it less resistant to electrophilic as well as to nucleophilic attacks.

On the other hand, as a result of the favorably dissipated electron density, **3** possesses a highly symmetrical structure having no possibilities for the attack of nucleophiles and electrophiles. This, coupled with the high conformational energy barrier, makes **3** very suitable for the fixation of tritium on a molecular basis.

(22) Since protonated nitrogens do not invert, the conformational change would proceed by what Simons and Park termed homeomorphic isomerization, which involves the passage of one bridge through the ring formed by the other two bridges.

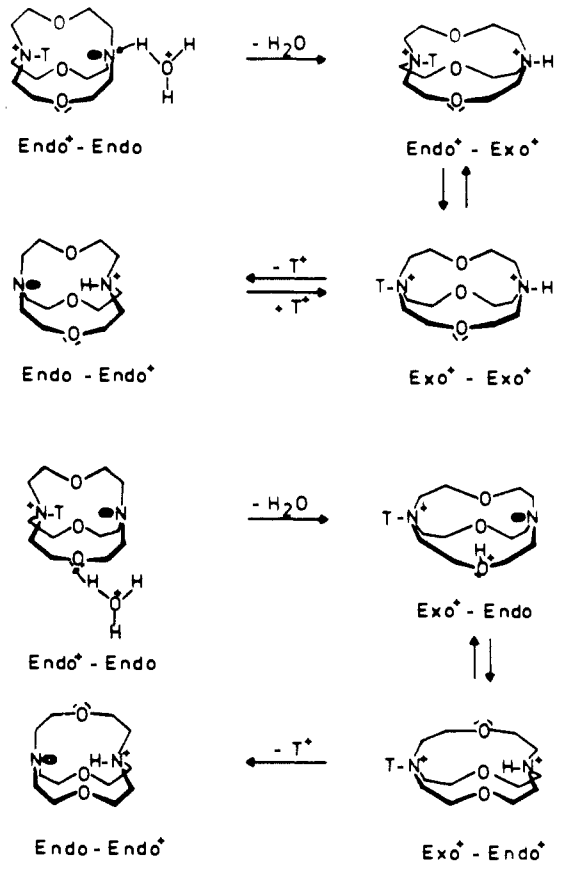

Figure 6. Plausible mechanism of tritium exchange in **2**.

Table V. Crystal and Data Collection Parameters for Cryptand 111 and Its Protonated Products

	111 **1**	[111-H] Picrate **2**	[111-2H] Picrate **3**
formula	$C_{12}H_{24}N_2O_3$	$C_{12}H_{25}N_2O_3^+$-$C_6H_2N_3O_7^-$	$C_{12}H_{26}N_2O_3^{2+}$-$2C_6H_2N_3O_7^-$
formula wt	244	473	702
crystal system	monoclinic	monoclinic	triclinic
space group	C_c	$P2_1/n$	$P\bar{1}$
Z	4	4	2
D_{calcd}, g/cm^3	1.23	1.448	1.38
10^9V, pm^3	1.309	2.17	1.663
a, pm	1304 (8)	1183.9 (4)	1377.8 (1)
b, pm	1164 (7)	781.7 (2)	1184.4 (1)
c, pm	872 (3)	2371.0 (9)	1165.8 (1)
α, deg	90	90	118.97 (1)
β, deg	99.88 (1)	98.38 (1)	93.73 (1)
γ, deg	90	90	91.56 (1)
radiation	Mo Kα	Cu Kα	Cu Kα
fract. angle, deg	$5 < 2\theta < 60$	$3 < 2\theta < 56$	$2.5 < 2\theta < 50$
$F(000)$	536	1000	536
no. of refl. measd.	1923	3843	5443
indep. refl.	1560	2762	3303
R	0.079	0.0918	0.062
R_w	0.051	0.059	0.081

To the best of our knowledge, **3** is hitherto the only compound with such properties.

3. Experimental Section

The cryptand 111 was obtained from Merck, Darmstadt, FRG, and purified by recrystallization. D_2O and DCl were also obtained from Merck. Tritium was provided free of charge as HTO in D_2O solution by the Kernforschungszentrum Karlsruhe, FRG. The specific activities were up to 29.6 GBq/mL (0.8 Ci/mL).

Tritium activities were measured by the liquid scintillation technique in a Packard Tricarb 2524 under internal standardization and employment of the cocktail Miniria 20 obtained from Zinsser, Frankfurt, FRG.

Infrared spectra were run as Nujol mull on the spectrometers PE 325 and PE 598 of Perkin-Elmer, Ltd.

Protonation, deuteration, and tritiation were performed as described by Lehn.[8]

For the X-ray structure analyses, the following programs were used: MULTAN 77,[23] X-RAY-76,[24] SHELX-75,[25] ABWI,[26] and XANADU.[27]

Table V shows important data of the crystal structure determination of the investigated complexes.

Acknowledgment. We gratefully acknowledge the financial support by the Bundesministerium für Forschung und Technologie as well as the Verband der Chemischen Industrie—Fonds der Chemischen Industrie.

(23) Main, P.; Lessinger, L.; Woolfson, M. M.; Germann, G.; Declerq, J. P. "MULTAN 77"; Universities of York, England and Louvain, Belgium, 1977.
(24) Stewart, K. M. "The X-RAY-76 System"; Computer Science Center, University of Maryland: College Park, MD, 1976; Technical Report, TR 446.
(25) Sheldrick, G. "Programs for Crystal Structure Determination"; Cambridge University Press: New York, 1975.
(26) Hoffmann, K. Dissertation, Universität Hamburg, 1976.
(27) Robert, P.; Sheldrick, G. "XANADU Program for Crystallographic Calculation"; Cambridge University Press: New York, 1975; p 975.

Hydrolysis of the Model Carcinogen *N*-(Pivaloyloxy)-4-methoxyacetanilide: Involvement of *N*-Acetyl-*p*-benzoquinone Imine

Michael Novak,* Maria Pelecanou, and Lee Pollack

Contribution from the Department of Chemistry, Clark University, Worcester, Massachusetts 01610. *Received August 6, 1985*

Abstract: Results of kinetic, ^{1}H NMR, and HPLC studies show that *N*-(pivaloyloxy)-4-methoxyacetanilide (**1a**), a model for suspected carcinogenic metabolites of phenacetin (**10**), decomposes predominately into *N*-acetyl-*p*-benzoquinone imine (**3**) in aqueous solution. The only other product isolated from the decomposition of **1a** is 4-methoxyacetanilide (**7**), which is produced in moderate yield at pH > 6.0. The available evidence indicates that both of these materials are produced by a nitrenium ion mechanism. In aqueous solutions containing KCl at pH < 6.0, **3** decomposes in a first-order manner by an acid-catalyzed process into *p*-benzoquinone (**6**) and 3-chloro-4-hydroxyacetanilide (**5**). An intermediate in the reaction, which decomposes into **6**, has been detected. ^{1}H NMR results indicate that the intermediate is a carbinolamine (**8**). At pH > 6.0, the decomposition of **3** becomes very complicated. At high concentrations, **3** decomposes by a non-first-order path into a material which appears to be oligomeric. At sufficiently low concentrations (ca. 2.5×10^{-6} M), the decomposition of **3** returns to a first-order process. Under these conditions, the major products of the reaction are **6** and acetaminophen (**4**). The measured standard reduction potential for **3** of 0.978 ± 0.001 V indicates that it is a much stronger oxidizing agent than either *p*-benzoquinone or *p*-benzoquinone monoimine. However, at this time it is not possible to determine the identity of the species responsible for the reduction of **3** into **4** in aqueous solution.

As part of a study of the chemistry of model compounds for the proximate carcinogenic metabolites of aromatic amides,[1] we have been investigating the aqueous solution chemistry of a series of ring-substituted *N*-(pivaloyloxy)- and *N*-(sulfonatooxy)acetanilides (**1** and **2**).[2] These compounds decompose in aqueous

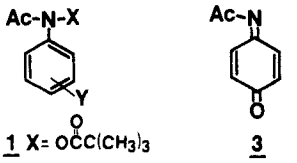

solution through the intermediacy of nitrenium ion pairs.[2] During our studies, we have obtained indirect evidence that *N*-acetyl-*p*-benzoquinone imine, **3**, may be involved in some of the decomposition pathways of these species if the ring substituent, Y, is at the 4-position and is a good leaving group.[2a,c] We have proposed that **3** may be formed by attack of H_2O at the 4-position of the nitrenium ion intermediate with subsequent loss of HY, as in eq 1.[2a] However, no direct evidence for such a process was obtained.

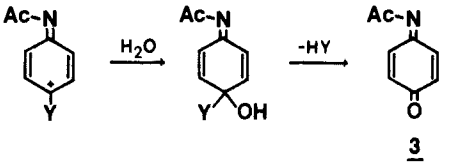

(1)

We can now report direct evidence based on kinetic studies and, ^{1}H NMR and HPLC experiments, that one member of this series of compounds, *N*-(pivaloyloxy)-4-methoxyacetanilide, **1a**, decomposes in aqueous solution between pH 3.0 and 8.0 predominately (>80%) through the intermediacy of **3**. As part of this

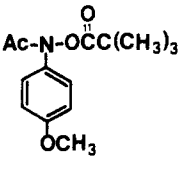

1a

study, we have investigated the hydrolysis and redox chemistry of **3** in this pH region. These results are also reported in this paper.

N-Acetyl-*p*-benzoquinone imine, **3**, is apparently an important hepatotoxic metabolite of the common analgesics acetaminophen[3]

(1) Miller, J. A. *Cancer Res.* **1970**, *30*, 559-576. Kriek, E. *Biochim. Biophys. Acta* **1974**, *355*, 177-203. Miller, E. C. *Cancer Res.* **1978**, *38*, 1479-1496. Miller, E. C.; Miller, J. A. *Cancer* **1981**, *47*, 2327-2345.
(2) (a) Novak, M.; Pelecanou, M.; Roy, A. K.; Andronico, A. F.; Plourde, F. M.; Oleflowicz, T. M.; Curtin, T. J. *J. Am. Chem. Soc.* **1984**, *106*, 5623-5631. (b) Novak, M.; Roy, A. K. *J. Org. Chem.* **1985**, *50*, 571-580. (c) Pelecanou, M.; Novak, M. *J. Am. Chem. Soc.* **1985**, *107*, 4499-4503. (d) Novak, M.; Roy, A. K. *J. Org. Chem.*, in press.
(3) (a) Blair, I. A.; Boobis, A. R.; Davies, D. S. *Tetrahedron Lett.* **1980**, *21*, 4947-4950. (b) Dahlin, D. C.; Nelson, S. D. *J. Med. Chem.* **1982**, *25*, 885-886. (c) Miner, D. J.; Kissinger, P. T. *Biochem. Pharmacol.* **1979**, *28*, 3285-3290. (d) Dahlin, D. C.; Miwa, G. T.; Lu, A. Y. H.; Nelson, S. D. *Proc. Natl. Acad. Sci. U.S.A.* **1984**, *81*, 1327-1331. (e) Corcoran, G. B.; Mitchell, J. R.; Vaishnav, Y. N.; Horning, E. C. *Molec. Pharmacol.* **1980**, *18*, 536-542.

0002-7863/86/1508-0112$01.50/0